Decay of inertial waves in rotating fluids

Andrey A. Gelash[1,2]†, Victor S. L'vov[3] and Vladimir E. Zakharov[1,4,5]

[1]Novosibirsk State University, Novosibirsk, 630090, Russia

[2]Kutateladze Institute of Thermophysics, SB RAS, Novosibirsk, 630090, Russia

[3]Department of Chemical Physics, The Weizmann Institute of Science, Rehovot, 76100, Israel

[4]Department of Mathematics, University of Arizona, AZ 857201 Tucson, USA

[5]Lebedev Physical Institute, Russian Academy of Sciences, Moscow, 119991, Russia

(Received xx; revised xx; accepted xx)

We build the Hamiltonian formalism for inertial waves in rotating incompressible fluid. We calculate and study in details the resonance three-wave interaction Hamiltonian. In the case of rapid rotation three-wave interactions play the key role in the weakly nonlinear wave dynamic. We investigate decay instability, confluence of two waves and discuss the future applications of the Hamiltonian approach in the theory of inertial waves.

1. Introduction

Rotation can fundamentally change the behavior of fluids flows. The presence of the Coriolis force leads to emerging of special type of waves – inertial waves (Greenspan 1968). Such waves appear in geophysical, astrophysical and industrial flows. In an incompressible fluid rotating with angular velocity $\boldsymbol{\Omega}$ inertial waves have the following dispersion law:

$$\omega_{\boldsymbol{k}} = 2\Omega|\cos\theta_{\boldsymbol{k}}|\,. \tag{1.1}$$

Here $\theta_{\boldsymbol{k}}$ is the angle between wave vector $\boldsymbol{k}$ and the angular velocity vector $\boldsymbol{\Omega}$. The linear theory of inertial waves was well studied (Landau & Lifshitz 1987). This waves propagate inside the volume of the fluid and have circular polarization. The special attention attract their unusual properties of reflection from the rigid boundary (Greenspan 1968). Note, that plane inertial wave is exact solution of the fully nonlinear Euler equations. This fact will be discussed in the first paragraph.

Real physical rotating flows can be complicated by influence of other factors such as gravitation or electromagnetic force (in the last case the fluid should be an electric conductor); the angular velocity of the fluid can depend from radius etc. Then the dispersion law is more tricky than eq. (1.1) (Le Gal 2013). Other important effects are due to the nonlinear wave interactions.

The degree of nonlinearity is characterized by parameter δ which can be obtained from the Euler equations in the rotating reference frame as follows:

$$\delta \equiv \frac{|[\boldsymbol{u}, \operatorname{rot}\boldsymbol{u}]|}{|[\boldsymbol{\Omega}, \boldsymbol{u}]|}\,. \tag{1.2}$$

Here $\boldsymbol{u}$ is the velocity fluctuations (in our case the characteristic value of the wave amplitude). In this work we assume that *nonlinearity parameter is small:* $\delta \ll 1$, i.e. waves interact weakly. It means that we can try to construct a perturbation theory, where n-wave interactions are the terms of perturbation series. The first nonlinear term in this series corresponds to three-wave interactions. They can be allowed (so called

† Email address for correspondence: agelash@gmail.com

resonance interaction) or forbidden (*nonresonance* interactions) by conservation laws. The dispersion law 1.1 allows three-wave interaction processes for inertial waves, i.e. corresponding momentum and energy conservation laws have nonzero set of solutions in $\boldsymbol{k}$-space, which is called a resonance surface. It means that inertial waves belong to "*the decay type*". This determines in many aspects their nonlinear behavior (see the monograph of Zakharov *et al.* (1992)).

Hamiltonian formalism is the most straightforward and general way to study weakly nonlinear wave systems without dissipation (Zakharov & Kuznetsov 1997). Recently the Hamiltonian formalism was developed for similar problem of internal waves in stratified nonrotating fluids (Lvov & Tabak 2001) which allowed to explain some features of wave energy spectra in the ocean (Lvov *et al.* 2004). A Hamiltonian nature of the Euler equation for incompressible fluid is known at least since a middle of the last century, including the case of rotating fluid (see the monograph of Lamb (1945)). In more recent time this fact was discussed by Morrison (1998) and by Salmon (1988). So, the problem is mainly technical: how to introduce a canonical variables for rotating fluid by the most convenient way for the description of inertial wave interactions?

In this work we find canonical variables which give an enormous technical advantage for calculating interaction Hamiltonian for inertial waves. Note, that we do not consider vortexes and other complicated flows so the Clebsch variables provide "one-to-one correspondence" with physical variables (which reference is the best here??). We focus on the decay of the wave $\boldsymbol{k}_1$ to the waves $\boldsymbol{k}_2$ and $\boldsymbol{k}_3$, which satisfy the following momentum and energy conservation laws:

$$\boldsymbol{k}_1 = \boldsymbol{k}_2 + \boldsymbol{k}_3, \tag{1.3a}$$

$$\omega_{\boldsymbol{k}_1} = \omega_{\boldsymbol{k}_2} + \omega_{\boldsymbol{k}_3}. \tag{1.3b}$$

As well known this decay is unstable: amplitudes of the waves $\boldsymbol{k}_2$ and $\boldsymbol{k}_3$ can grow exponentially, so this process is called *decay instability* (see for instance the first paragraph in the book (L'vov 1994)). The growth rate of the instability $\gamma(\boldsymbol{k}_1, \boldsymbol{k}_2, \boldsymbol{k}_3)$ depends on the amplitude of three-wave interaction $V^{\boldsymbol{k}_1}_{\boldsymbol{k}_2\boldsymbol{k}_3}$ and reaches its maximum at the resonance surface for the process (1.3).

The behavior of the growth increment play one of the key role for weakly nonlinear dynamic and statistic of inertial waves which can be investigated in numerical and natural experiments. In the present work we study in details the growth increment $\gamma(\boldsymbol{k}_1, \boldsymbol{k}_2, \boldsymbol{k}_3)$ on the resonance surface. The resonance surface for inertial waves has nontrivial form with branches at $k \to \infty$ (Bellet *et al.* 2006). We find that the increment at this branches is nonzero, what means that instability can develop for shortwave perturbations up to the dissipative threshold. Finally we derive the simple approximation for three-wave amplitude in small frequency limit and study another three-wave process of waves confluence: $\boldsymbol{k}_1 + \boldsymbol{k}_2 \to \boldsymbol{k}_3$. Thus, we build the Hamiltonian formalism for inertial waves in rotating fluid and describe the main three-wave processes.

2. Inertial waves of finite amplitude in rotating fluids

In the reference frame rotating with the incompressible fluid the Euler equations are (Landau & Lifshitz 1987):

$$\partial_t \boldsymbol{v} + (\boldsymbol{v} \cdot \boldsymbol{\nabla})\boldsymbol{v} + 2(\boldsymbol{\Omega} \times \boldsymbol{v}) = -\boldsymbol{\nabla} P, \tag{2.1a}$$

$$\boldsymbol{\nabla} \cdot \boldsymbol{v} = 0, \tag{2.1b}$$

where $\boldsymbol{\Omega}$ is the angular velocity. The term $2(\boldsymbol{\Omega} \times \boldsymbol{v})$ is the Coriolis force. The term P is the effective pressure, which includes the fluid pressure p and the centrifugal force: $P = p - \frac{1}{2}(\boldsymbol{\Omega} \times \boldsymbol{r})^2$. The equation of continuity (2.1b) is the same as in nonrotating case.

Here and below we work only in the rotating reference frame. Let us denote coordinates in this frame as (x, y, z) and the corresponding unit vectors as $\widehat{\boldsymbol{x}}$, $\widehat{\boldsymbol{y}}$, $\widehat{\boldsymbol{z}}$. In the paper we assume that angular velocity is directed along $\widehat{\boldsymbol{z}}$:

$$\boldsymbol{\Omega} = (0, 0, \Omega)\,. \tag{2.2}$$

The plane inertial wave of finite amplitude is the exact solution of the Euler equations (2.1). The wavepacked of inertial waves also is the exact solution of (2.1), i.e. only the waves propagating in different directions can interact nonlinearly. This fact is not properly discuss in the literature (except the paper of Messio *et al.* (2008)). In this paragraph we obtain the plane wave as a general solution of the Euler equations (2.1) in assumption that the velocity field depends only on one coordinate ξ along arbitrary direction $\boldsymbol{n}$:

$$\boldsymbol{v} = \boldsymbol{v}(\xi)\,, \qquad \boldsymbol{n} = (\sin\theta, 0, \cos\theta). \tag{2.3}$$

In this case the Euler equations (2.1) become linear. Indeed, if we assume that fluid velocity vanish on the infinity:

$$\boldsymbol{v}(\xi) \to 0 \quad \text{at} \quad \xi \to \infty\,, \tag{2.4}$$

the nonlinear term in (2.1a) is exactly canceled:

$$(\boldsymbol{v}(\xi) \cdot \boldsymbol{\nabla})\boldsymbol{v}(\xi) = 0. \tag{2.5}$$

Now the Euler equations (2.1) can be written as the following system of linear equations:

$$\begin{aligned} \frac{\partial v_x}{\partial t} - 2\Omega v_y + \sin\theta \frac{\partial P}{\partial \xi} &= 0, \\ \frac{\partial v_y}{\partial t} + 2\Omega v_x &= 0, \\ \frac{\partial v_z}{\partial t} + \cos\theta \frac{\partial P}{\partial \xi} &= 0. \end{aligned} \tag{2.6}$$

This system of equations has the exact solution:

$$\begin{aligned} v_x &= A(\xi)\cos\theta\sin\omega t - B(\xi)\cos\theta\cos\omega t, \\ v_y &= A(\xi)\cos\omega t + B(\xi)\sin\omega t, \\ v_z &= -A(\xi)\sin\theta\sin\omega t + B(\xi)\sin\theta\cos\omega t. \end{aligned} \tag{2.7}$$

Here $\omega^2 = 4\Omega^2\cos^2\theta$ in line with our dispersion law (1.1). $A(\xi)$, $B(\xi)$ are the arbitrary functions of ξ, which, according to assumption (2.4), vanish on the infinity.

Solution (2.7) is the wave packet of plane inertial waves. Now we can introduce the wave vector $\boldsymbol{k}$ parallel to $\mathbf{n}$. If we choose $A(\xi) = -A\sin(\boldsymbol{k}\cdot\boldsymbol{r})$, $B(\xi) = A\cos(\boldsymbol{k}\cdot\boldsymbol{r})$ we obtain well-known circularly polarized plane wave solution (Landau & Lifshitz 1987):

$$\begin{aligned} v_{0x} &= -A\cos\theta_{\boldsymbol{k}}\sin(\omega_{\boldsymbol{k}}t - \boldsymbol{k}\cdot\boldsymbol{r}), \\ v_{0y} &= A\sin(\omega_{\boldsymbol{k}}t - \boldsymbol{k}\cdot\boldsymbol{r}), \\ v_{0z} &= A\sin\theta_{\boldsymbol{k}}\sin(\omega_{\boldsymbol{k}}t - \boldsymbol{k}\cdot\boldsymbol{r}). \end{aligned} \tag{2.8}$$

Thus, we derive the inertial wave (2.8) as exact solution of the Euler equations (2.1), i.e. without any assumption about wave amplitude A.

3. Hamiltonian description of inertial waves

3.1. *Clebsch representation for the velocity field*

It is well-known that the Euler equations for incompressible nonrotating fluid can be written as a Hamiltonian system using so called Clebsch variables $\lambda(\boldsymbol{r},t)$ and $\mu(\boldsymbol{r},t)$ (Lamb 1945). We find the following Clebsch representation for the velocity field corresponding the Euler equations (2.1):

$$\boldsymbol{v}(\boldsymbol{r},t) = \sqrt{2\Omega}\big[\widehat{\boldsymbol{y}}\lambda(\boldsymbol{r},t) - \widehat{\boldsymbol{x}}\mu(\boldsymbol{r},t)\big] + \lambda(\boldsymbol{r},t)\boldsymbol{\nabla}\mu(\boldsymbol{r},t) + \boldsymbol{\nabla}\Phi(\boldsymbol{r},t)\ . \tag{3.1}$$

Here we assume that angular velocity is defined as in Eq. (2.3). The last two terms in (3.1) correspond to standard Clebsch representation. They contain the potential $\Phi(\boldsymbol{r},t)$, which can be uniquely determined from the proper boundary conditions and the incompressibility condition (2.1b). The first term appear as a result of transition to the rotating coordinate system. Note that similar variables were introduced by Zakharov (1971) in the theory of magnetized plasma (or by Kuznetsov in another paper??).

Alternatively $\boldsymbol{v}(\boldsymbol{r},t)$ can be written using transverse projector $\widehat{\mathbf{P}} \equiv 1 - \boldsymbol{\nabla}\Delta^{-1}\boldsymbol{\nabla}$ as:

$$\boldsymbol{v} = \widehat{\mathbf{P}} \cdot \left[\sqrt{2\Omega}\,(\lambda\widehat{\boldsymbol{y}} - \mu\widehat{\boldsymbol{x}}) + \lambda\boldsymbol{\nabla}\mu\right]\ . \tag{3.2}$$

The fields $\lambda(\boldsymbol{r},t)$ and $\mu(\boldsymbol{r},t)$ are not determined uniquely for a given velocity field $\boldsymbol{v}(\boldsymbol{r},t)$. For instance, transformation

$$\lambda(\boldsymbol{r},t) \to a\lambda(\boldsymbol{r},t) + b\,, \qquad \mu(\boldsymbol{r},t) \to \mu(\boldsymbol{r},t)/a + c\,,$$

where a, b, and c are arbitrary constants, does not change the field $\boldsymbol{v}$. This kind of the "gauge invariance" of the Clebsch transformation allows to select special calibration of $\lambda(\boldsymbol{r},t)$ and $\mu(\boldsymbol{r},t)$, which is most appropriate for a solution of a particular problem. Of course, equations for $\lambda(\boldsymbol{r},t)$ and $\mu(\boldsymbol{r},t)$ will depend on the calibration.

Fields $\lambda(\boldsymbol{r},t)$, $\mu(\boldsymbol{r},t)$ obey Hamiltonian equations of motion in the canonical form:

$$\partial_t\lambda = \frac{\delta\mathcal{H}}{\delta\mu}\,, \qquad \partial_t\mu = -\frac{\delta\mathcal{H}}{\delta\lambda}\,, \tag{3.3}$$

where the Hamiltonian $\mathcal{H}$ is the energy represented via λ and μ:

$$\mathcal{H} = \int \frac{1}{2}|\boldsymbol{v}|^2 d\boldsymbol{r}\ . \tag{3.4}$$

Equations (3.3) and (3.4) yield:

$$\partial_t\lambda = -(\boldsymbol{v}\cdot\boldsymbol{\nabla})\lambda - \sqrt{2\Omega}v_x\,, \tag{3.5a}$$

$$\partial_t\mu = -(\boldsymbol{v}\cdot\boldsymbol{\nabla})\mu - \sqrt{2\Omega}v_y\ . \tag{3.5b}$$

From Eqs. (3.1) and (3.5) we find that $\boldsymbol{v}$ really satisfies the Euler equations (2.1) with the effective pressure

$$P = -\partial_t\Phi - \lambda\partial_t\mu - \frac{1}{2}|\boldsymbol{v}|^2 - \frac{1}{2}(\boldsymbol{\Omega}\times\boldsymbol{r})^2\ . \tag{3.6}$$

More rigorously representation (3.1) can be obtained by direct transition to rotated reference frame. We will perform it for the general case of elliptic flows in our next work.

3.2. *Hamiltonian in rotating reference frame*

Let us introduce the following notations for the velocity field (3.1):

$$\boldsymbol{v} = \boldsymbol{v}_1 + \boldsymbol{v}_2, \qquad \boldsymbol{v}_1 = \widehat{\mathbf{P}} \cdot \left[\sqrt{2\Omega}(\lambda\widehat{\boldsymbol{y}} - \mu\widehat{\boldsymbol{x}})\right], \qquad \boldsymbol{v}_2 = \widehat{\mathbf{P}} \cdot (\lambda\boldsymbol{\nabla}\mu), \tag{3.7}$$

and symmetric Fourier transform:

$$\boldsymbol{v}_{\boldsymbol{k}} = \frac{1}{(2\pi)^{3/2}} \int \boldsymbol{v}(\boldsymbol{r}) \exp(-i\boldsymbol{k}\cdot\boldsymbol{r}) d\boldsymbol{r}, \quad \boldsymbol{v} = \frac{1}{(2\pi)^{3/2}} \int \boldsymbol{v}_{\boldsymbol{k}} \exp(i\boldsymbol{k}\cdot\boldsymbol{r}) d\boldsymbol{k}\,. \tag{3.8}$$

Now according to Eq. (3.4) the Hamiltonian can be written as a sum of the following three terms:

$$\mathcal{H} = \mathcal{H}_2 + \mathcal{H}_3 + \mathcal{H}_4\,. \tag{3.9}$$

Here

$$\mathcal{H}_2 = \frac{1}{2}\int |\boldsymbol{v}_{1\boldsymbol{k}}|^2 d\boldsymbol{k}\ , \tag{3.10a}$$

$$\mathcal{H}_3 = \frac{1}{2}\int (\boldsymbol{v}_{1\boldsymbol{k}}\cdot\boldsymbol{v}_{2\boldsymbol{k}} + \boldsymbol{v}^*_{1\boldsymbol{k}}\cdot\boldsymbol{v}_{2\boldsymbol{k}}) d\boldsymbol{k}\,, \tag{3.10b}$$

$$\mathcal{H}_4 = \int |\boldsymbol{v}_{2\boldsymbol{k}}|^2 d\boldsymbol{k}\,. \tag{3.10c}$$

The interactions of inertial waves are described by the last two terms in Eq. (3.9). We denote them as *interaction Hamiltonian*:

$$\mathcal{H}_{int} = \mathcal{H}_3 + \mathcal{H}_4\,. \tag{3.11}$$

Note that (3.9) is the exact Hamiltonian for our problem. It contains finite number of terms since for the incompressible flow we use only one pair of canonical variables $\lambda(\boldsymbol{r},t)$ and $\mu(\boldsymbol{r},t)$.

Now let us denote:

$$\boldsymbol{k} = (k_x, k_y, k_z) = (k\sin\theta\cos\varphi, k\sin\theta\sin\varphi, k\cos\theta), \qquad \boldsymbol{k}_\perp = (k_x, k_y). \tag{3.12}$$

Using the expression for transverse projector in $\boldsymbol{k}$-space:

$$\widehat{P}^{\alpha\beta}_{\boldsymbol{k}} = \delta^{\alpha\beta} - \frac{k^\alpha k^\beta}{k^2}, \tag{3.13}$$

we calculate according to Eq. (3.7) the vectors:

$$\boldsymbol{v}_{1\boldsymbol{k}} = \sqrt{2\Omega}\big[\lambda_{\boldsymbol{k}}\widehat{\boldsymbol{y}} - \mu_{\boldsymbol{k}}\widehat{\boldsymbol{x}} - \frac{\boldsymbol{k}}{k^2}\big(k_y\lambda_{\boldsymbol{k}} - k_x\mu_{\boldsymbol{k}}\big)\big], \tag{3.14a}$$

$$\boldsymbol{v}_{2\boldsymbol{k}} = \frac{i}{(2\pi)^{3/2}}\int \Big(\boldsymbol{k}_2 - \boldsymbol{k}\frac{\boldsymbol{k}\cdot\boldsymbol{k}_2}{k^2}\Big)\lambda_{\boldsymbol{k}_1}\mu_{\boldsymbol{k}_2}\delta_{\boldsymbol{k}-\boldsymbol{k}_1-\boldsymbol{k}_2} d\boldsymbol{k}_1 d\boldsymbol{k}_2\,. \tag{3.14b}$$

Note, that $\boldsymbol{v}_{2\boldsymbol{k}} = 0$ when $\boldsymbol{k}||\boldsymbol{k}_1||\boldsymbol{k}_2$. In this case $\mathcal{H}_{int} = 0$. It means that inertial waves moving in one direction do not interact as we discussed at the beginning.

3.3. *Canonical form of the quadratic Hamiltonian*

Now we introduce canonical transformation of the Clebsch variables in $\boldsymbol{k}$-space:

$$\mu_{\boldsymbol{k}} = \widetilde{\mu}_{\boldsymbol{k}}\cos\varphi + \widetilde{\lambda}_{\boldsymbol{k}}\sin\varphi = \frac{1}{k_\perp}\big(\widetilde{\mu}_{\boldsymbol{k}}k_x + \widetilde{\lambda}_{\boldsymbol{k}}k_y\big)\,, \tag{3.15}$$

$$\lambda_{\boldsymbol{k}} = -\widetilde{\mu}_{\boldsymbol{k}}\sin\varphi + \widetilde{\lambda}_k\cos\varphi = \frac{1}{k_\perp}\big(-\widetilde{\mu}_{\boldsymbol{k}}k_y + \widetilde{\lambda}_{\boldsymbol{k}}k_x\big)\,.$$

After this transformation it is easy to find normal variables $c_{\boldsymbol{k}}$ and $c^*_{\boldsymbol{k}}$:

$$\widetilde{\mu}_{\boldsymbol{k}} = \sqrt{\frac{\Omega}{\omega_{\boldsymbol{k}}}}(c_{\boldsymbol{k}} + c^*_{-\boldsymbol{k}})\,, \quad \widetilde{\lambda}_{\boldsymbol{k}} = -\frac{i}{2}\sqrt{\frac{\omega_{\boldsymbol{k}}}{\Omega}}(c_{\boldsymbol{k}} - c^*_{-\boldsymbol{k}})\,, \tag{3.16}$$

which allow us to write quadratic Hamiltonian in the diagonal form:

$$\mathcal{H}_2 = \int \omega_{\boldsymbol{k}} c_{\boldsymbol{k}} c^*_{\boldsymbol{k}} d\boldsymbol{k}\,, \quad \omega_{\boldsymbol{k}} = 2\Omega|\cos\theta_{\boldsymbol{k}}| \tag{3.17}$$

3.4. *Interaction Hamiltonian*

We calculate three-wave interaction Hamiltonian in two steps. Firstly we calculate $\mathcal{H}_3$ in variables $\widetilde{\mu}_{\boldsymbol{k}}$ and $\widetilde{\lambda}_{\boldsymbol{k}}$ according to Eq. (3.10b), Eq. (3.14a), Eq. (3.14b) and Eq. (3.15). After symmetrization $\mathcal{H}_3$ becomes explicitly invariant under rotation by azimuth angle φ:

$$\begin{aligned}\mathcal{H}_3 = \frac{i\sqrt{2\Omega}}{2(2\pi)^{3/2}} \int \frac{d\boldsymbol{k}_1 d\boldsymbol{k}_2 d\boldsymbol{k}_3}{k_{1\perp}k_{2\perp}k_{3\perp}} \delta_{\boldsymbol{k}_1-\boldsymbol{k}_2-\boldsymbol{k}_3}\big(F^{\boldsymbol{k}_1}_{\boldsymbol{k}_2\boldsymbol{k}_3}\mu_{\boldsymbol{k}_1} - S_{\boldsymbol{k}_2\boldsymbol{k}_3}\lambda_{\boldsymbol{k}_1}\big) \\ \times\Big[S_{\boldsymbol{k}_2\boldsymbol{k}_3}(\mu_{\boldsymbol{k}_2}\mu_{\boldsymbol{k}_3} + \lambda_{\boldsymbol{k}_2}\lambda_{\boldsymbol{k}_3}) + (\boldsymbol{k}_{2\perp}\cdot\boldsymbol{k}_{3\perp})(\mu_{\boldsymbol{k}_2}\lambda_{\boldsymbol{k}_3} - \lambda_{\boldsymbol{k}_2}\mu_{\boldsymbol{k}_3})\Big].\end{aligned} \tag{3.18}$$

Here

$$\begin{aligned}F^{\boldsymbol{k}_1}_{\boldsymbol{k}_2\boldsymbol{k}_3} &= \frac{1}{2}\Big[k^2_{1\perp}\frac{\boldsymbol{k}_1\cdot\boldsymbol{k}_2 - \boldsymbol{k}_1\cdot\boldsymbol{k}_3}{k_1^2} + k^2_{2\perp} - k^2_{3\perp}\Big], \\ S_{\boldsymbol{k}_2\boldsymbol{k}_3} &= k_{3x}k_{2y} - k_{2x}k_{3y} = k_{2\perp}k_{3\perp}\sin(\varphi_2-\varphi_3).\end{aligned} \tag{3.19}$$

Note that

$$F^{\boldsymbol{k}_i}_{\boldsymbol{k}_l\boldsymbol{k}_m} = -F^{\boldsymbol{k}_i}_{\boldsymbol{k}_m\boldsymbol{k}_l}, \qquad S_{\boldsymbol{k}_l\boldsymbol{k}_m} = -S_{\boldsymbol{k}_m\boldsymbol{k}_l}, \qquad S_{\boldsymbol{k}_2,\boldsymbol{k}_3} = S_{\boldsymbol{k}_3,\boldsymbol{k}_1} = S_{\boldsymbol{k}_1,\boldsymbol{k}_2}. \tag{3.20}$$

Then we substitute normal variables Eq. (3.16) in (3.18) and after symmetrization $\mathcal{H}_3$ takes the standard form:

$$\begin{aligned}\mathcal{H}_3 = \frac{1}{2}\int (V^{\boldsymbol{k}_1}_{\boldsymbol{k}_2\boldsymbol{k}_3} c^*_{\boldsymbol{k}_1} c_{\boldsymbol{k}_2} c_{\boldsymbol{k}_3} + c.c)\delta_{\boldsymbol{k}_1-\boldsymbol{k}_2-\boldsymbol{k}_3} d\boldsymbol{k}_1 d\boldsymbol{k}_2 d\boldsymbol{k}_3 + \\ + \frac{1}{6}\int (U_{\boldsymbol{k}_1\boldsymbol{k}_2\boldsymbol{k}_3} c^*_{\boldsymbol{k}_1} c^*_{\boldsymbol{k}_2} c^*_{\boldsymbol{k}_3} + c.c.)\delta_{\boldsymbol{k}_1+\boldsymbol{k}_2+\boldsymbol{k}_3} d\boldsymbol{k}_1 d\boldsymbol{k}_2 d\boldsymbol{k}_3\,.\end{aligned} \tag{3.21}$$

where

$$\begin{aligned}U_{\boldsymbol{k}_1\boldsymbol{k}_2\boldsymbol{k}_3} = -\frac{3i\sqrt{2\Omega}}{(2\pi)^{3/2}k_{1\perp}k_{2\perp}k_{3\perp}}\Big\{-\sqrt{\frac{\Omega^3}{\omega_{\boldsymbol{k}_1}\omega_{\boldsymbol{k}_2}\omega_{\boldsymbol{k}_3}}}F^{\boldsymbol{k}_1}_{\boldsymbol{k}_2\boldsymbol{k}_3}S_{\boldsymbol{k}_3\boldsymbol{k}_2} \\ + \frac{i}{8}\sqrt{\frac{\omega_{\boldsymbol{k}_1}\omega_{\boldsymbol{k}_2}\omega_{\boldsymbol{k}_3}}{\Omega^3}}S_{\boldsymbol{k}_3\boldsymbol{k}_2} + \frac{1}{4}\sqrt{\frac{\omega_{\boldsymbol{k}_2}\omega_{\boldsymbol{k}_3}}{\Omega\,\omega_{\boldsymbol{k}_1}}}F^{\boldsymbol{k}_1}_{\boldsymbol{k}_2\boldsymbol{k}_3}S_{\boldsymbol{k}_3\boldsymbol{k}_2} \\ - \frac{i}{2}\sqrt{\frac{\Omega\,\omega_{\boldsymbol{k}_1}}{\omega_{\boldsymbol{k}_2}\omega_{\boldsymbol{k}_3}}}S^2_{\boldsymbol{k}_3\boldsymbol{k}_2} - \frac{i}{2}\sqrt{\frac{\Omega\,\omega_{\boldsymbol{k}_3}}{\omega_{\boldsymbol{k}_1}\omega_{\boldsymbol{k}_2}}}F^{\boldsymbol{k}_1}_{\boldsymbol{k}_2\boldsymbol{k}_3}(\boldsymbol{k}_{2\perp}\cdot\boldsymbol{k}_{3\perp}) \\ + \frac{i}{2}\sqrt{\frac{\Omega\,\omega_{\boldsymbol{k}_2}}{\omega_{\boldsymbol{k}_1}\omega_{\boldsymbol{k}_3}}}F^{\boldsymbol{k}_1}_{\boldsymbol{k}_2\boldsymbol{k}_3}(\boldsymbol{k}_{2\perp}\cdot\boldsymbol{k}_{3\perp}) + \frac{1}{4}\sqrt{\frac{\omega_{\boldsymbol{k}_1}\omega_{\boldsymbol{k}_3}}{\Omega\,\omega_{\boldsymbol{k}_2}}}S_{\boldsymbol{k}_3\boldsymbol{k}_2}(\boldsymbol{k}_{2\perp}\cdot\boldsymbol{k}_{3\perp}) \\ - \frac{1}{4}\sqrt{\frac{\omega_{\boldsymbol{k}_1}\omega_{\boldsymbol{k}_2}}{\Omega\,\omega_{\boldsymbol{k}_3}}}S_{\boldsymbol{k}_3\boldsymbol{k}_2}(\boldsymbol{k}_{2\perp}\cdot\boldsymbol{k}_{3\perp})\Big\}.\end{aligned} \tag{3.22}$$

$$V^{\boldsymbol{k}_1}_{\boldsymbol{k}_2\boldsymbol{k}_3} = \frac{i\sqrt{2\Omega}}{(2\pi)^{3/2}k_{1\perp}k_{2\perp}k_{3\perp}}\Big\{\sqrt{\frac{\Omega^3}{\omega_{\boldsymbol{k}_1}\omega_{\boldsymbol{k}_2}\omega_{\boldsymbol{k}_3}}}S_{\boldsymbol{k}_3\boldsymbol{k}_2}\big[F^{\boldsymbol{k}_1}_{\boldsymbol{k}_2\boldsymbol{k}_3} - F^{\boldsymbol{k}_2}_{\boldsymbol{k}_1\boldsymbol{k}_3} - F^{\boldsymbol{k}_3}_{\boldsymbol{k}_2\boldsymbol{k}_1}\big] \quad (3.23)$$

$$-\frac{3i}{8}\sqrt{\frac{\omega_{\boldsymbol{k}_1}\omega_{\boldsymbol{k}_2}\omega_{\boldsymbol{k}_3}}{\Omega^3}}S^2_{\boldsymbol{k}_3\boldsymbol{k}_2} + \frac{i}{2}\sqrt{\frac{\Omega}{\omega_{\boldsymbol{k}_1}\omega_{\boldsymbol{k}_2}\omega_{\boldsymbol{k}_3}}}(\omega_{\boldsymbol{k}_1}-\omega_{\boldsymbol{k}_2}-\omega_{\boldsymbol{k}_3})S^2_{\boldsymbol{k}_3\boldsymbol{k}_2}$$

$$+\frac{1}{4}\sqrt{\frac{\omega_{\boldsymbol{k}_2}\omega_{\boldsymbol{k}_3}}{\Omega\,\omega_{\boldsymbol{k}_1}}}S_{\boldsymbol{k}_3\boldsymbol{k}_2}\big[-F^{\boldsymbol{k}_1}_{\boldsymbol{k}_2\boldsymbol{k}_3} + \boldsymbol{k}_{1\perp}\cdot\boldsymbol{k}_{3\perp} - \boldsymbol{k}_{1\perp}\cdot\boldsymbol{k}_{2\perp}\big]$$

$$-\frac{i}{2}\sqrt{\frac{\Omega\,\omega_{\boldsymbol{k}_1}}{\omega_{\boldsymbol{k}_2}\omega_{\boldsymbol{k}_3}}}\big[-F^{\boldsymbol{k}_3}_{\boldsymbol{k}_2\boldsymbol{k}_1}(\boldsymbol{k}_{1\perp}\cdot\boldsymbol{k}_{2\perp}) + F^{\boldsymbol{k}_2}_{\boldsymbol{k}_1\boldsymbol{k}_3}(\boldsymbol{k}_{1\perp}\cdot\boldsymbol{k}_{3\perp})\big]$$

$$-\frac{i}{2}\sqrt{\frac{\Omega\,\omega_{\boldsymbol{k}_3}}{\omega_{\boldsymbol{k}_1}\omega_{\boldsymbol{k}_2}}}\big[-F^{\boldsymbol{k}_1}_{\boldsymbol{k}_2\boldsymbol{k}_3}(\boldsymbol{k}_{2\perp}\cdot\boldsymbol{k}_{3\perp}) + F^{\boldsymbol{k}_2}_{\boldsymbol{k}_1\boldsymbol{k}_3}(\boldsymbol{k}_{1\perp}\cdot\boldsymbol{k}_{3\perp})\big]$$

$$-\frac{i}{2}\sqrt{\frac{\Omega\,\omega_{\boldsymbol{k}_2}}{\omega_{\boldsymbol{k}_1}\omega_{\boldsymbol{k}_3}}}\big[F^{\boldsymbol{k}_1}_{\boldsymbol{k}_2\boldsymbol{k}_3}(\boldsymbol{k}_{2\perp}\cdot\boldsymbol{k}_{3\perp}) - F^{\boldsymbol{k}_3}_{\boldsymbol{k}_2\boldsymbol{k}_1}(\boldsymbol{k}_{1\perp}\cdot\boldsymbol{k}_{2\perp})\big]$$

$$-\frac{1}{4}\sqrt{\frac{\omega_{\boldsymbol{k}_1}\omega_{\boldsymbol{k}_3}}{\Omega\,\omega_{\boldsymbol{k}_2}}}S_{\boldsymbol{k}_3\boldsymbol{k}_2}\big[F^{\boldsymbol{k}_2}_{\boldsymbol{k}_1\boldsymbol{k}_3} + \boldsymbol{k}_{2\perp}\cdot\boldsymbol{k}_{3\perp} + \boldsymbol{k}_{1\perp}\cdot\boldsymbol{k}_{2\perp}\big]$$

$$+\frac{1}{4}\sqrt{\frac{\omega_{\boldsymbol{k}_1}\omega_{\boldsymbol{k}_2}}{\Omega\,\omega_{\boldsymbol{k}_3}}}S_{\boldsymbol{k}_3\boldsymbol{k}_2}\big[-F^{\boldsymbol{k}_3}_{\boldsymbol{k}_2\boldsymbol{k}_1} + \boldsymbol{k}_{2\perp}\cdot\boldsymbol{k}_{3\perp} + \boldsymbol{k}_{1\perp}\cdot\boldsymbol{k}_{3\perp}\big]\Big\}$$

The amplitude $V^{\boldsymbol{k}_1}_{\boldsymbol{k}_2\boldsymbol{k}_3}$ describes the three-wave processes of decay and confluence which we study in the next paragraphs. The amplitude $U_{\boldsymbol{k}_1\boldsymbol{k}_2\boldsymbol{k}_3}$ corresponds to the so called *explosive three-wave instability*. Explosive instability appears when waves with negative energy can propagate in the medium. We do not consider this case in the paper. (Is it possible in rotating fluid??)

4. Resonance surface

In this paragraph we study resonance conditions for the processes of wave decay: $\boldsymbol{k}_1 \to \boldsymbol{k}_2 + \boldsymbol{k}_3$ and wave confluence: $\boldsymbol{k}_1 + \boldsymbol{k}_2 \to \boldsymbol{k}_3$. Let us assume that the value of vector $\boldsymbol{k}_1$ is fixed. Thus we have only two free parameters. Indeed, to satisfy the decay momentum conservation law (1.3a) we can write wave vectors as follows:

$$\begin{aligned}\boldsymbol{k}_1 &= (k_1\sin\theta_1\ ,0\ ,k_1\cos\theta_1),\\ \boldsymbol{k}_2 &= (k_1\sin\theta_1 - k_{3x}\ ,-k_{3y}\ ,k_1\cos\theta_1 - k_{3z}).\\ \boldsymbol{k}_3 &= (k_{3x}\ ,k_{3y}\ ,k_{3z}),\end{aligned} \quad (4.1)$$

Now using the energy conservation law (1.3b) and the dispersion relation (1.1) we obtain the following resonance condition:

$$|k_1\cos\theta_1| = \frac{|k_{3z}|}{\sqrt{k^2_{3x}+k^2_{3y}+k^2_{3z}}} + \frac{|k_1 cos\theta_1 - k_{3z}|}{\sqrt{(k_1\sin\theta_1 - k_{3x})^2 + k^2_{3y} + (k_1\cos\theta_1 - k_{3z})^2}} \quad (4.2)$$

This expression defines the set of vectors $\boldsymbol{k}_3$ which give the main contribution to the decay processes. The coordinates of the vector $\boldsymbol{k}_2$ form the two-dimensional resonance surface in $\boldsymbol{k}$-space.

We solve (4.2) numerically by using "Mathematica" (Wolfram Research). On the Fig. 1 we present the example of resonance surface and its two-dimensional cut at certain

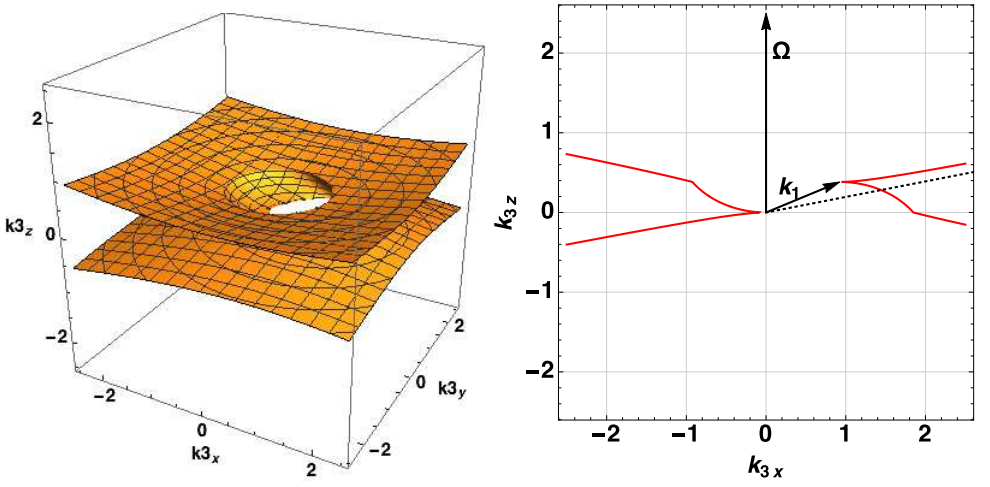

FIGURE 1. Left: resonance surface of the wave vector $\boldsymbol{k}_3$ for the decay process $\boldsymbol{k}_1 \to \boldsymbol{k}_2 + \boldsymbol{k}_3$. The initial wave vector $\boldsymbol{k}_1 = (\sin\frac{\pi}{4}, 0, \cos\frac{\pi}{4})$. Right: cut of this surface (resonance curve) at $\varphi_3 = 0$.

azimuth angle φ_3 (see 3.12) – the *resonance curve*. In the decay process the energy of initial wave $\boldsymbol{k}_1$ is bigger then the energy of any *secondary wave* $\boldsymbol{k}_2$ or $\boldsymbol{k}_3$. Thus, according to the dispersion relation (1.1) angles θ_2 and θ_3 are always closer to $\pi/2$ than θ_1 as shown on the Fig. 1.

The resonance surface for inertial waves has nontrivial form with branches at $k \to \infty$ Bellet *et al.* (2006). It means that in the theory the wavelength of secondary waves can be arbitrary small. In real systems the minimal wavelength is limited by dissipation rate or boundary conditions. We find the following asymptotics for the infinite branches assuming in (4.2) $k_3 \to \infty$:

$$\frac{|k_1 \cos\theta_1|}{2} = \frac{|k_{3z}|}{\sqrt{k_{3x}^2 + k_{3y}^2 + k_{3z}^2}} \tag{4.3}$$

We plot one of this asymptotics on the Fig. 1 by a dashed line.

Using equations similar to (4.1) and (4.2) we find resonance surface for the process of wave confluence. On the Fig. 2 we plot resonance surface and resonance curve for the vector $\boldsymbol{k}_3$. Confluence resonance surface is finite in $\boldsymbol{k}$-space and grow when θ_1 tends to $\pi/2$. Note, that the resonance surface for vector $\boldsymbol{k}_2$ has similar form, thus we do not present it here.

5. Growth rate of decay instability

As well known the decay $\boldsymbol{k}_1 \to \boldsymbol{k}_2 + \boldsymbol{k}_3$ is unstable. Let amplitudes of secondary waves $A_{\boldsymbol{k}_2}$ and $A_{\boldsymbol{k}_3}$ be small in comparison with the amplitude of the initial wave $A_{\boldsymbol{k}_1}$ at $t = 0$: $A_{\boldsymbol{k}_1}(0) \gg max(|A_{\boldsymbol{k}_2}(0)|, |A_{\boldsymbol{k}_3}(0)|)$. According to the well known theory (which reference is the best??), at the linear stage the amplitudes of secondary waves growth as ($A_{\boldsymbol{k}_1} \sim const$):

$$A_{\boldsymbol{k}_{2,3}}(t) = A_{\boldsymbol{k}_{2,3}}(0) e^{\lambda t} \tag{5.1}$$

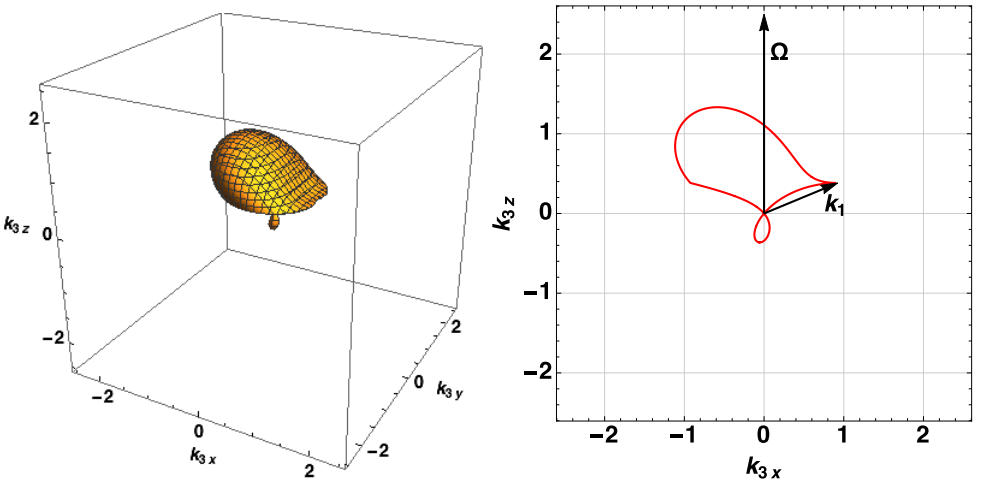

FIGURE 2. Left: resonance surface of the wave vector $\boldsymbol{k}_3$ for the confluence process $\boldsymbol{k}_1 + \boldsymbol{k}_2 \to \boldsymbol{k}_3$. The initial wave vector $\boldsymbol{k}_1 = (\sin\frac{\pi}{4}, 0, \cos\frac{\pi}{4})$. Right: resonance curve at $\varphi_3 = 0$.

where

$$\lambda = \frac{i}{2}(\omega_{\boldsymbol{k}_1} - \omega_{\boldsymbol{k}_2} - \omega_{\boldsymbol{k}_3}) + \left[4|V^{\boldsymbol{k}_1}_{\boldsymbol{k}_2\boldsymbol{k}_3}|^2|A_{\boldsymbol{k}_1}|^2 - \frac{(\omega_{\boldsymbol{k}_1} - \omega_{\boldsymbol{k}_2} - \omega_{\boldsymbol{k}_3})^2}{4}\right]^{1/2}. \tag{5.2}$$

The increment of growth

$$\gamma = \left[4|V^{\boldsymbol{k}_1}_{\boldsymbol{k}_2\boldsymbol{k}_3}|^2|A_{\boldsymbol{k}_1}|^2 - \frac{(\omega_{\boldsymbol{k}_1} - \omega_{\boldsymbol{k}_2} - \omega_{\boldsymbol{k}_3})^2}{4}\right]^{1/2} \tag{5.3}$$

is localized in the layer of thickness $8|V^{\boldsymbol{k}_1}_{\boldsymbol{k}_2\boldsymbol{k}_3}|^2|A_k(0)|^2$ near the resonance surface (4.2) where it reaches the following maximum value:

$$2|V^{\boldsymbol{k}_1}_{\boldsymbol{k}_2\boldsymbol{k}_3}||A_k(0)|. \tag{5.4}$$

In this paragraph we study absolute value of the three-wave decay amplitude $|V^{\boldsymbol{k}_1}_{\boldsymbol{k}_2\boldsymbol{k}_3}|$ (3.23) at the resonance surface (4.2). It is enough to describe the main features of the growth increment behavior.

On the Fig. 3 we present the typical examples of resonance surface colored corresponding to the value of $|V^{\boldsymbol{k}_1}_{\boldsymbol{k}_2\boldsymbol{k}_3}|$. We find that the decay amplitude has nonzero value on the infinite branches. We calculate the following asymptotic expression of $V^{\boldsymbol{k}_1}_{\boldsymbol{k}_2\boldsymbol{k}_3}$ on the upper infinite branch of resonance surface using (3.23) and (4.1), (4.2), (4.3):

$$V^{\boldsymbol{k}_1}_{\boldsymbol{k}_2\boldsymbol{k}_3}(\varphi_3) \xrightarrow[\omega_{\boldsymbol{k}_1}=\omega_{\boldsymbol{k}_2}+\omega_{\boldsymbol{k}_3}]{k_3\to\infty} \frac{i\sqrt{2\Omega}}{(2\pi)^{3/2}}\left\{-\frac{1}{4}\sqrt{\frac{\omega_{\boldsymbol{k}_1}}{\Omega}}\sin\varphi_3\cos\varphi_3\sin\theta_1\left(1+\frac{5}{16}\frac{\omega^2_{\boldsymbol{k}_1}}{\Omega^2}\right)\right. \tag{5.5}$$

$$-\frac{1}{2}\sqrt{\frac{\Omega}{\omega_{\boldsymbol{k}_1}}}\frac{\sin\varphi_3\cos\theta_1}{\sqrt{1-\frac{\omega^2_{\boldsymbol{k}_1}}{16\Omega^2}}}\left(1-\frac{11}{16}\frac{\omega^2_{\boldsymbol{k}_1}}{\Omega^2}+\frac{5}{128}\frac{\omega^4_{\boldsymbol{k}_1}}{\Omega^4}\right)$$

$$-\frac{3i}{16}\left(\frac{\omega_{\boldsymbol{k}_1}}{\Omega}\right)^{3/2}\sqrt{1-\frac{\omega^2_{\boldsymbol{k}_1}}{4\Omega^2}}\sin^2\varphi_3+\frac{i}{2}\left(\frac{\omega_{\boldsymbol{k}_1}}{4\Omega}\sin\theta_1\cos\varphi_3-\sqrt{1-\frac{\omega^2_{\boldsymbol{k}_1}}{16\Omega^2}}\cos\theta_1\right)$$

$$\left.\times\left[\frac{3}{2}\sqrt{\frac{\omega_{\boldsymbol{k}_1}}{\Omega}}\cos\varphi_3-\sqrt{\frac{\Omega}{\omega_{\boldsymbol{k}_1}}\left(1-\frac{\omega^2_{\boldsymbol{k}_1}}{16\Omega^2}\right)}\left(\frac{\omega_{\boldsymbol{k}_1}}{\Omega}\sqrt{1-\frac{\omega^2_{\boldsymbol{k}_1}}{16\Omega^2}}\cos\varphi_3-\cos\theta_1\sin\theta_1\right)\right]\right\}$$

It means that instability may appear for shortwave perturbations up to the dissipative threshold with the increment described by (5.4) and (5.5). Note, that to obtain asymptotics for the lower infinite branch we need to change $\varphi_3 \to \varphi_3 + \pi$ in Eq. (5.5). We present the dependence $|V^{\boldsymbol{k}_1}_{\boldsymbol{k}_2\boldsymbol{k}_3}(\varphi_3)|$ corresponding to (5.5) for different values of initial vector $\boldsymbol{k}_1$ on the Fig. 4. This asymptotics is almost isotropic by angle φ_3 when θ_1 is small. When θ_1 is close to $\pi/2$ the value of $|V^{\boldsymbol{k}_1}_{\boldsymbol{k}_2\boldsymbol{k}_3}(\varphi_3)|$ became smaller and anysotropic with maximum near $\varphi_3 = \pi/4,\, 3\pi/4$.

As we can see from the Fig. 1 right (or left) part of the resonance curve can be presented as a function of k_{3z}. Thus, it is convenient to plot the values of $|V^{\boldsymbol{k}_1}_{\boldsymbol{k}_2\boldsymbol{k}_3}|$ corresponding (3.23) along one part of the resonance curve - see the Fig. 5.

Finally we discuss the case of especial interest for the wave turbulence theory. To date it is well established that statistical behavior of inertial waves in rapidly rotating fluids is highly anisotropic (see for instance the book of Nazarenko (2011) and references herein). The dispersion law (1.1) leads to the formation of energy cascade predominantly in $\boldsymbol{k}_\perp$ - direction when the wave frequencies are small. The weak turbulent energy spectra for inertial waves was found by Galtier (2003). We find the following asymptotics for $V^{\boldsymbol{k}_1}_{\boldsymbol{k}_2\boldsymbol{k}_3}$ is the small frequency limit:

$$V^{\boldsymbol{k}_1}_{\boldsymbol{k}_2\boldsymbol{k}_3} \approx \frac{i}{16\pi^{3/2}} \frac{S_{\boldsymbol{k}_2\boldsymbol{k}_3}}{k_{1\perp}k_{2\perp}k_{3\perp}\sqrt{\omega_{\boldsymbol{k}_1}\omega_{\boldsymbol{k}_2}\omega_{\boldsymbol{k}_3}}} \tag{5.6}$$
$$\times\left[\omega^2_{\boldsymbol{k}_1}(k^2_{3\perp} - k^2_{2\perp}) + \omega^2_{\boldsymbol{k}_2}(k^2_{1\perp} - k^2_{3\perp}) - \omega^2_{\boldsymbol{k}_3}(k^2_{1\perp} - k^2_{2\perp})\right]$$

One of the most natural and effective types of energy pumping for the wave turbulent cascade can be produced by the phenomena of parametric instability (see the book of L'vov (1994)). For inertial waves in rotating fluid such instability was first discovered by Bayly (1986). He shown that small ellipticity of the flow leads to excitation of parametric waves with maximum increment at angles θ_p satisfying the condition:

$$|\cos\theta_p| = \frac{1}{2}. \tag{5.7}$$

On the Fig. 6 we check how the asymptotics (5.6) works at really small frequencies ($\theta \sim \frac{\pi}{2}$) and the *pumping frequency*:

$$\omega_p = 2\Omega|\cos\theta_p|. \tag{5.8}$$

We find that for the latter case asymptotics (5.6) works well only in the middle branch of the resonance surface. We will discuss this fact in our next work devoted to the turbulence of inertial waves under parametric excitation.

6. Conclusion

In this paper we have developed Hamiltonian formalism for inertial waves in rotating fluid and studied the resonance three-wave interaction processes. Special attention we have paid to the decay $\boldsymbol{k}_1 \to \boldsymbol{k}_2 + \boldsymbol{k}_3$, which is responsible for the decay instability and plays central role in the formation of wave turbulence spectrum. We have studied geometry of the resonance surface as well as increment of the instability. We have calculated several asymptotics of the matrix element which help to understand main characteristics of the instability and can be useful for future study of wave turbulence problem.

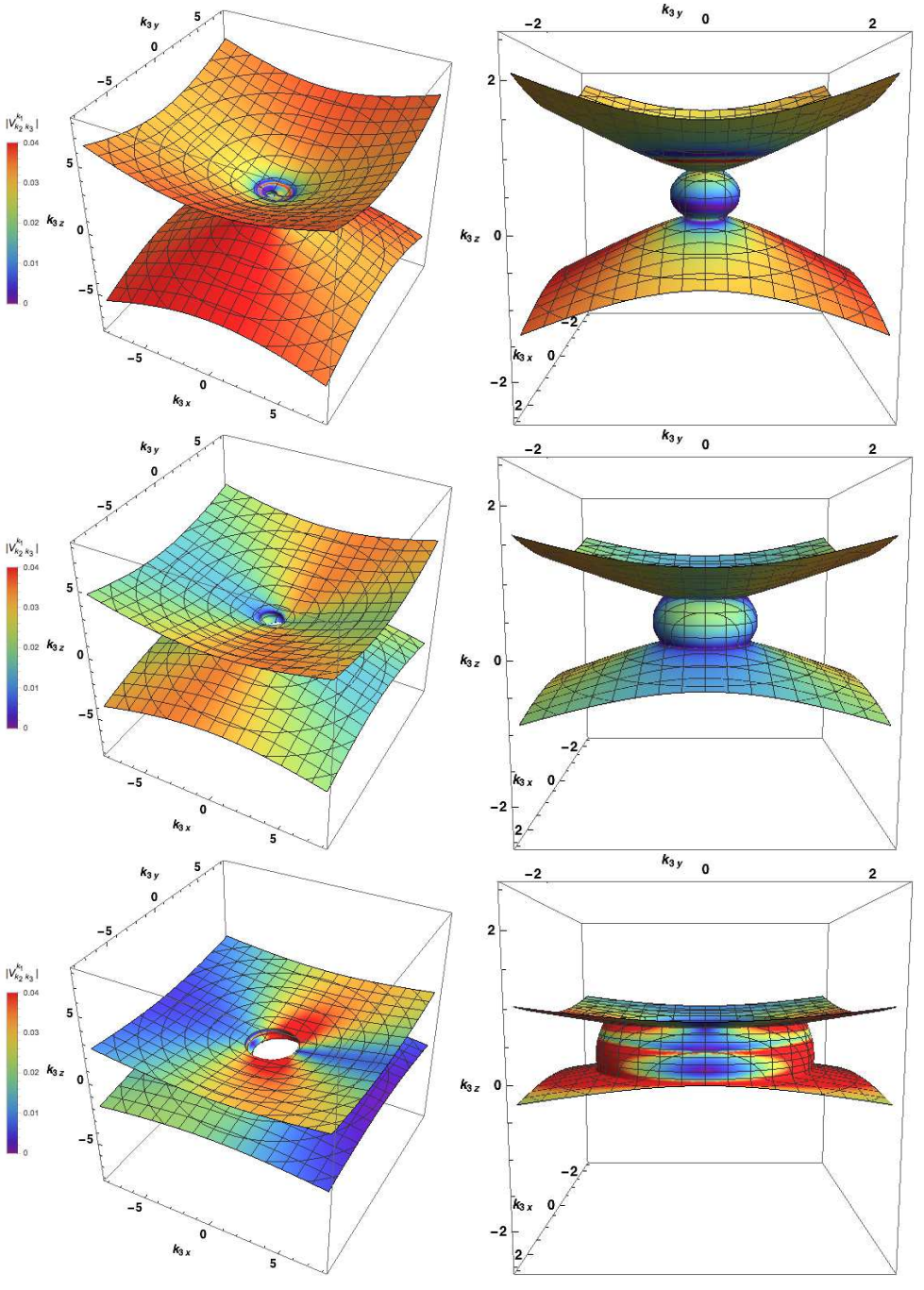

FIGURE 3. Resonance surface of the wave vector $\boldsymbol{k}_3$ for the decay process $\boldsymbol{k}_1 \to \boldsymbol{k}_2 + \boldsymbol{k}_3$. The surface colored corresponding to the value of $|V^{\boldsymbol{k}_1}_{\boldsymbol{k}_2\boldsymbol{k}_3}|$, for different directions of initial wave: $\theta = \frac{\pi}{8}$ (top row), $\theta = \frac{\pi}{4}$ (middle row), $\theta = \frac{3\pi}{8}$ (bottom row). Left and right pictures demonstrate the same surface at different scales and view points.

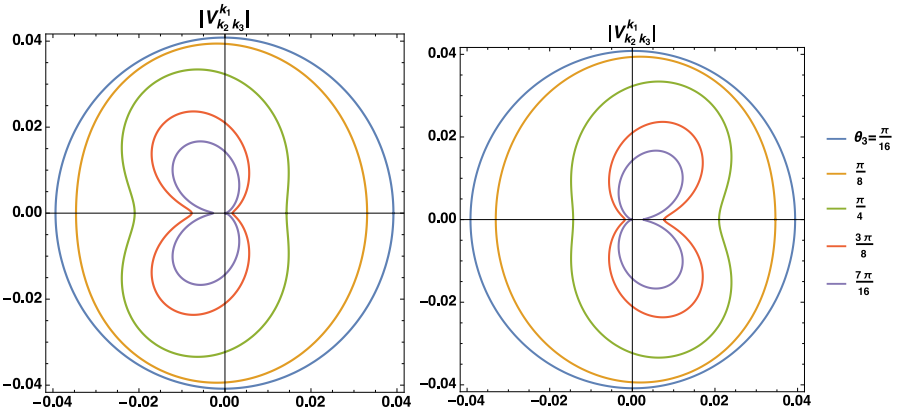

FIGURE 4. Asymptotic values of $|V^{k_1}_{k_2k_3}(\varphi_3)|$ on the resonance surface at $k_3 \to \infty$ for different directions of initial wave. Left - the lower infinite branch of resonance surface, right - the upper infinite branch.

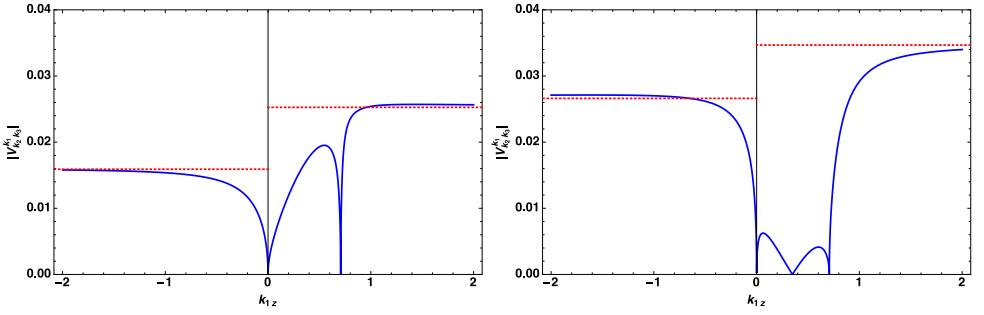

FIGURE 5. Typical behavior of $|V^{k_1}_{k_2k_3}|$ (blue solid lines) on the resonance curve corresponding different values of φ_1. The directions of initial wave $\theta_1 = \frac{\pi}{4}$. Left: $\varphi_1 = \frac{\pi}{8}$, the amplitude has a local maximum at the middle branch of the resonance curve and minimum at the point when one branch of the resonance curve changes to another, then it approaches asymptotic values 5.5 (red dotted lines). Right: $\varphi_1 = \frac{\pi}{8}$ the growth increment has two local maximum and additional minimum at the middle branch of the resonance curve.

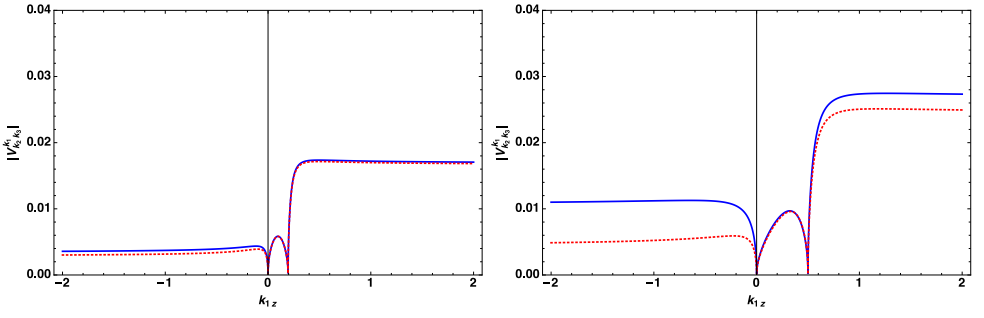

FIGURE 6. Comparison of $|V^{k_1}_{k_2k_3}|$ given by (3.23) (blue solid lines) and its small-frequency asymptotics given by (5.6) (red dashed lines). Left (small frequency): $\theta = \frac{7\pi}{16}, \varphi_1 = \frac{\pi}{4}$. Right (pumping frequency): $\theta = \theta_p, \varphi_1 = \frac{\pi}{4}$.

We expect that described features of weakly nonlinear behavior can be directly observed in numerical simulation. In natural experiments the precise measurement of such nonlinear effects for inertial waves is not trivial problem. Early we have mentioned that inertial waves in rotating fluids and internal waves in stratified fluids are similar. Indeed, the dispersion law for internal waves is $\omega_{\boldsymbol{k}} = \omega_0 |\sin\theta_{\boldsymbol{k}}|$, where constant ω_0 is the so called *buoyancy frequency* and $\theta_{\boldsymbol{k}}$ is the angle between wave vector and the direction of stratification (Phillips 1966), thus this two types of waves have analogous three wave resonance interaction. Recently developed experimental technique based on the properties of reflection of internal waves from the rigid boundary allows to focus waves and study nonlinear effects of the wave interaction (Scolan *et al.* 2013; Brouzet *et al.* To be published). Inertial waves have similar reflection properties, therefore we hope that similar experiments for this type of waves are also possible.

Note that despite similar features of inertial and internal waves, the Hamiltonian formalism is significantly different for this two problems. Unlike the case of internal waves here we use Clebsch variables and transition to rotating reference frame.

In this paper we assume the presence of small parameter δ (1.2) and neglect the four-wave processes. Indeed, the three-wave interaction brings the main contribution to weak nonlinear dynamics and defines energy cascade for wave turbulence. However, for some problems four-wave interaction plays the central role. The excellent example here is the parametric wave turbulence. The corresponding theory was introduced by V.E. Zakharov, V.S. L'vov and S.S. Starobinets (Zakharov *et al.* (1971)) for spin waves. They shown that four-wave interactions conserve phase correlation within each parametrically excited pair of waves, which eventually leads to the particular "phase" mechanism of wave amplitude saturation. As was mentioned at the end of the last paragraph for inertial waves the role of parametric pumping plays small ellipticity of the flow. Our next paper will be devoted to this subject.

7. Acknowledgments

The study of the growth rate of thee-wave instability was performed by supporting of the Russian Science Foundation (Grand No. 14-22-00174). AG also thanks support of the RFBR (Grant No. 16-31-60086 mol a dk). VL thanks??

REFERENCES

Bayly, B. J. 1986 Three-dimensional instability of elliptical flow. *Physical review letters* **57** (17), 2160.

Bellet, F., Godeferd, F. S., Scott, J. F. & Cambon, C. 2006 Wave turbulence in rapidly rotating flows. *Journal of Fluid Mechanics* **562**, 83–121.

Brouzet, C., Sibgatullin, I., Scolan, H., Ermanyuk, E. & Dauxois, T. To be published Internal wave attractors examined using laboratory experiments and 3d numerical simulations. *Journal of Fluid Mechanics* .

Galtier, S. 2003 Weak inertial-wave turbulence theory. *Physical Review E* **68** (1), 015301.

Greenspan, H. P. 1968 *The theory of rotating fluids Cambridge University Press*. Cambridge, England.

Lamb, H. 1945 *Hydrodynamics*. Dover, New York.

Landau, L. D. & Lifshitz, E. M. 1987 *Fluid Mechanics*. Pergamon Press, Oxford.

Le Gal, P. 2013 Waves and instabilities in rotating and stratified flows. In *Fluid Dynamics in Physics, Engineering and Environmental Applications*, pp. 25–40. Springer.

L'vov, Victor S. 1994 *Wave turbulence under parametric excitation*. Springer, Berlin, Heidelberg.

Lvov, Yuri V., Polzin, Kurt L. & Tabak, Esteban G. 2004 Energy spectra of the ocean's internal wave field: Theory and observations. *Physical review letters* **92** (12), 128501.

Lvov, Yuri V. & Tabak, Esteban G. 2001 Hamiltonian formalism and the garrett-munk spectrum of internal waves in the ocean. *Physical review letters* **87** (16), 168501.

Messio, L., Morize, C., Rabaud, M. & Moisy, F. 2008 Experimental observation using particle image velocimetry of inertial waves in a rotating fluid. *Experiments in Fluids* **44** (4), 519–528.

Morrison, Philip J. 1998 Hamiltonian description of the ideal fluid. *Reviews of modern physics* **70** (2), 467.

Nazarenko, S. 2011 *Wave turbulence*. Springer Science Business Media.

Phillips, O. M. 1966 The dynamics of the upper ocean. *Cambridge University Press, Cambridge, England* .

Salmon, R. 1988 Hamiltonian fluid mechanics. *Annual review of fluid mechanics* **20** (1), 225–256.

Scolan, H., Ermanyuk, E. & Dauxois, T. 2013 Nonlinear fate of internal wave attractors. *Physical review letters* **110** (23), 234501.

Zakharov, V. E. 1971 Hamiltonian formalism for hydrodynamic plasma models. *Sov. Phys. JETP* **33**, 927–932.

Zakharov, V. E. & Kuznetsov, E. A. 1997 Hamiltonian formalism for nonlinear waves. *Physics-Uspekhi* **40** (11), 1087–1116.

Zakharov, V. E., L'vov, V. S. & Falkovich, G. 1992 *Kolmogorov spectra of turbulence 1. Wave turbulence.*, , vol. 1. Springer-Verlag, Berlin (Germany).

Zakharov, V. E., L'vov, V. S. & Starobinets, S. S. 1971 Stationary nonlinear theory of parametric excitation of waves. *Sov. Phys. JETP* **32**, 656.